Title

Analytic theory of L→H transition, barrier structure, and hysteresis for a simple model of coupled particle and heat fluxes

Journal

Physics of Plasmas, 15(12)

ISSN

1070-664X

Authors

Malkov, MA
Diamond, PH

Publication Date

2008-12-01

DOI

10.1063/1.3028305

Analytic theory of L→H transition, barrier structure, and hysteresis for a simple model of coupled particle and heat fluxes

M. A. Malkov and P. H. Diamond
Center for Astrophysics and Space Sciences and Department of Physics, University of California, San Diego, La Jolla, California 92093, USA

(Received 28 January 2008; accepted 29 October 2008; published online 3 December 2008)

The two-field (pressure/density) model for the L→H transition is extended and analyzed qualitatively. In its original form the model is ambiguous as to the location of the transition within the range of bistability of particle and thermal fluxes. Here, the model is regularized by including (i) hyperdiffusion, (ii) time dependence, and (iii) curvature of the pressure profile. The regularizations (i)–(ii) agree and indicate that the Maxwell rule for the forward and back transition applies, as opposed to the maximum flux forward and minimum flux backward transition rules (which yields hysteresis) as suggested previously. Regarding (i)–(ii), simple models suggest that for a pressure gradient driven electric field shear bifurcation, the basic scale of the pedestal is inexorably tied to the particle fueling depth, which normally is the neutral penetration depth. There is no hysteresis predicted by the local model of transport suppression. However, the effect of pressure profile curvature (iii) changes these results substantially. When it dominates, the curvature effect reduces the transition threshold to the lower end of the range of heating power, which falls within the phase coexistence region for both forward and back transitions. This softens the transition threshold requirements. In this limit, the model with pressure curvature also predicts transitions which occur in regimes of flat density and driven exclusively by the temperature gradient. This allows the pedestal to extend beyond the fueling depth, and also allows some decoupling of density and pressure profiles. In a parameter range where the pressure curvature is less important the transition occurs somewhere between the above two limits. © *2008 American Institute of Physics*.
[DOI: 10.1063/1.3028305]

I. INTRODUCTION

A very important goal of magnetic confinement fusion is to understand the mechanisms for the edge[1] and internal[2] transport barrier formation. The physics of the L→H transition may very well be related to an abrupt change of the edge plasma stability. However, an intrinsic bistability[3] of the transport fluxes is a more plausible alternative to this scenario. Loosely put, the two stable branches correspond to the low (L) and high (H) confinement modes, respectively. The details of the mechanism for L→H transition remain controversial but nearly all candidates involve some variation on the theme of electric field shear E_r' leading to reduction or suppression of turbulence.[4,5] It is natural to think of L→H transition and profile problems as phase transition phenomena,[6] with the electric field shear E_r' as the order parameter.[7] Here, the L-mode is analogous to the disordered phase (i.e., one with weak E_r' and strong turbulence) while the H-mode is analogous to the ordered phase (i.e., strong E_r' shear and weak or negligible turbulence). The local L→H bifurcation is then naturally analogous to a phase transition (or, more precisely, the advance or expansion of a region of H-phase into a region of L-phase[8]), and the problem of understanding H-mode pedestal structure is analogous to understanding phenomena, such as phase separation in the coexistence region (i.e., as in spinodal decomposition[9]), or the expansion of one phase into another, etc. Of course, the most important questions are when and where the forward L→H transition and back-transition actually occur. These play an important role in setting the actual pedestal width, as they define the effective dynamical boundary of the enhanced confinement region.

To this end, significant insight has been gained by considering simple, bistable S-curve bifurcation models.[10–12] In such models, the variation of the system state (e.g., local density gradient) as a function of the control parameter (e.g., local diffusive flux) is represented by an S-figure with two stable branches which, respectively, correspond to the L and H modes. These are connected by an unstable branch or transition region (see Fig. 1). Of course, this approach is intrinsically somewhat unsatisfactory, for many reasons. These include:

(a) The fact that the edge barrier (L→H) transition is a two-field problem, and must be described in terms of density and temperature, at minimum. This is because the ion pressure gradient driven electric field shear is dependent on both the density and ion temperature profiles, and so is sensitive to both particle and (ion) heat sources. This is, of course also consistent with the empirical observations that the L→H transition has both a power and a density threshold.[13]

(b) The fact that the S-curve is, itself, a function of the local plasma parameters. While the radial variation of structure of the S-curve can be represented by considering a static folded surface, or flux-landscape[14] function $\Gamma(E_r', r)$, its time evolution cannot be described without a dynamical model.

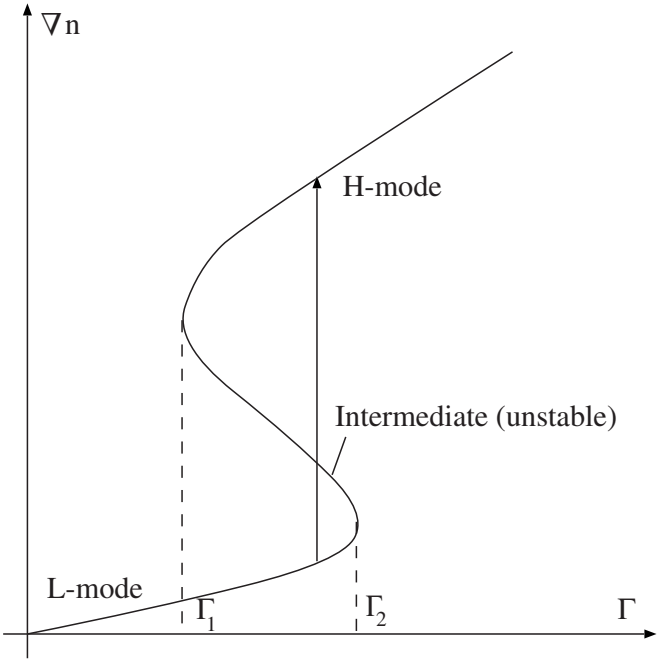

FIG. 1. Generic bifurcation diagram (S-curve) that illustrates a possible transition from the L (lower gradient) to H-mode (higher gradient) solution for a given particle deposition rate $\Gamma_1 < \Gamma < \Gamma_2$.

(c) The model is grossly oversimplified, and omits essentially all of the details of the transition dynamics, such as evolution of zonal flow[15–17] and mean poloidal and toroidal flows, interplay of fluctuation, flow and profile evolution, etc.[18,19] The model lumps all these phenomena into a simple bifurcation between the L-mode and an H-mode in which all fluctuations are quenched, and the residual transport is purely neoclassical. The effects of the radial variation of the transport coefficients are not addressed.

In spite of these shortcomings, the one-field S-curve paradigm has definitely furthered our understanding of the L→H bifurcation phenomena, as it captures many key aspects of the problem in a simple paradigmatic example. Moreover, there is some evidence that the experimentally determined flux versus. gradient plot is consistent with an S-curve bifurcation model.[20] However, it is also true that further progress now requires a new, improved model to be developed.

In this paper, we progress beyond the one field S-curve paradigm to consider a two-field transport bifurcation model, which describes the evolution of density n and pressure p. This model is solved analytically. It was proposed, but studied only numerically, by Hinton and Staebler.[11] Also, an *ad hoc* transition criterion was used in that work. We show this criterion to be invalid. The model employs a minimal model of E_r' suppression of turbulent thermal and particle transport. A simple substitution (diagonalization) reduces the coupled equations for density and pressure to two one-field bifurcation problems. Other than proximity to threshold, no simplifying assumptions or restrictions are invoked. We note that while independent equations for density and pressure are obtained, both particle and thermal source functions enter each

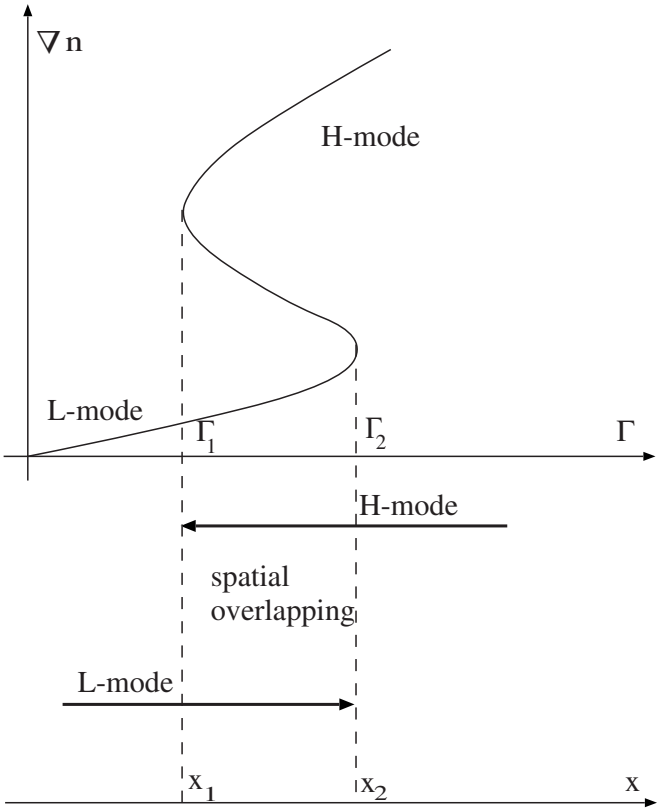

FIG. 2. The same as Fig. 1 but with the underlying alignment of L and H domains that may coexist in the interval $x_1 < x < x_2$.

equation. An exact criterion for phase coexistence (i.e., the possibility of bifurcation) is derived. While the model is a useful guide to the parameter study of L→H transitions, it does not, however, resolve the fundamental questions, which are of course (1) which of the two possible stable states does the system actually prefer, and (2) under what conditions do transitions between them occur? In the aforementioned spatial context, solution of this problem translates into determination of the exact position of the L→H interface and of the thickness of the plasma domain in which the state with the enhanced density and temperature gradients is established (i.e., the transport barrier or pedestal width). The thickness of the pedestal in turn, determines the improvement in the overall device performance through the enhancement of the density and temperature in the core plasma "contained" by the barrier, as well as the enhancement of the overall energy and particle confinement times (i.e., the H-factor).

Bistable systems are described by evolution equations whose stationary solutions are bivalued. While the underlying physics may be different in different systems, the very existence of a governing S-curve implies some aspects of universality in the dynamics. At the same time, a complete time dependent description is necessary to determine the time asymptotic state of a system. In other words, it is not clear *a priori* which of the two stable branches will be selected if the both are permissible stationary solutions for given values of control parameters.

This problem can be illustrated by an example, as follows (Fig. 2). Let us take the particle deposition rate Γ inside

a closed region as a control parameter, and the density gradient ∇n at its boundary as an order parameter. Note $\nabla n/n$ is related to E_r'. Clearly, as long as Γ is sufficiently small, so is the gradient ∇n, and the dependence $\nabla n(\Gamma)$ is unique. Thus, only one (L-mode) solution occurs. For growing Γ this changes, namely $\nabla n(\Gamma)$ becomes nonlinear and two additional solutions for $\nabla n(\Gamma)$ branch off at, say $\Gamma=\Gamma_1$, so that for $\Gamma_1<\Gamma<\Gamma_2$ three solutions are now possible. For $\Gamma>\Gamma_2$ only one (H-mode solution) remains. The intermediate solution is usually unstable, but the uppermost is stable and the transition to the upper branch may occur (theoretically) at any value of $\Gamma_1<\Gamma<\Gamma_2$. In low dimensional systems, such as electric circuits, where the control and order parameters are just simple time dependent variables, such as voltage and current, the transition occurs where one of the stable solutions simply no longer exists, i.e., in our case at Γ_2. Similarly, the reverse transition occurs when the upper solution disappears. In our case this happens when Γ goes below Γ_1. Obviously a hysteresis loop of the width $\Delta\Gamma=\Gamma_2-\Gamma_1$ in the particle flux forms in this case.

In continuous media (described by PDEs), where two states or phases can coexist in static, adjacent domains, this simple rule does not determine the L–H transition. To demonstrate this, suppose that $\Gamma(x)$ is monotonically increasing so that $\Gamma(x)>\Gamma_2=\Gamma(x_2)$ for $x>x_2$ (Fig. 2) and the above rule applies. Hence, the H-mode definitely occupies at least the half-space $x>x_2$. Since Γ decreases to the left, the transition H→L should occur (by the above rule) only at $x=x_1$, where $\Gamma(x_1)=\Gamma_1$. Now, a similar consideration can be repeated going from smaller to larger x. Namely, the L-mode must occupy the $x<x_1$ half-space and it should even persist up to $x=x_2$, where the L-branch disappears and the L→H transition must occur. This clearly contradicts our previous assertion that the region $x_1<x<x_2$ is occupied by the H-mode! There is no contradiction only for the trivial case $x_1=x_2$. Hence, the simple transition rule described above gives an ambiguous result for the transition location ($x=x_1$ or $x=x_2$). Alternatively put, this example shows that the actual location of the transition layer in the interval $[x_1,x_2]$ is indeterminate. This dilemma, while not explicitly discussed in Ref. 11, was de facto circumvented there by an additional *ad hoc* requirement that the jump in the density (or pressure) gradient across the transition should be the "least possible." This *ad hoc* rule happened to select $x=x_1$ as the transition point. Not only is this requirement arbitrary, but there are well known elementary examples where the opposite principle applies. For instance, in a flow with a coordinate dependent velocity profile, shocks form at such points so as to maximize the velocity jump across them and thus also maximize the efficiency of energy dissipation.

To summarize, the transition occurs anywhere within the phase coexistence interval $x_1<x<x_2$. Note that the model introduced in Ref. 11 and used below certainly admits that possibility. Therefore, further physical arguments are needed to determine the location of the transition.

The goal of this paper is thus twofold. First, we derive an exact criterion for phase coexistence. This will be achieved by obtaining a single "S-curve" by reducing the two coupled transport equations to two independent equations and then to a single combined equation for the product of the density and temperature gradients. Second, we consider temporal evolution and regularization of stationary equations to locate the transition point on the S-curve. One general and commonly used approach is to regularize the equations in the coexistence region by adding physically relevant regularization terms, such as a small hyperdiffusivity. For a flux driven, one field transport model, such a regularization has been performed in Ref. 8. It resulted in an "equal area," or Maxwell transition rule across the S-curve, similar to that in the shock formation or phase transition problems, and in contrast to the "maximum profile smoothness" principle suggested in Refs. 10 and 11. We also applied the hyperdiffusive regularization to the two field, distributed source driven model of Ref. 11. Not surprisingly, upon application to the diagonalized equations (i.e., which are in many respects similar to the one field model), this procedure also leads to the Maxwell rule for the transition location, as is shown in Sec. III B. However, the situation with the two field model is more complex. Indeed, a more consistent approach would be to add hyperdiffusive terms to both energy and particle transport equations prior to their diagonalization. This possibility was explored in detail by the late Rosenbluth.[21] He was able to prove that the transition point depends on the relation between the two regularizing coefficients. This is not an appealing result, and renders the whole regularization approach here dubious. Indeed, in general, the regularization implies that the transition point does not depend on the regularizing coefficient as long as it is small. Put more rigorously, the solution must converge to a unique weak solution of the original equation as the regularizing parameter tends to zero. Now that we need two regularization parameters (particle and heat hyperdiffusivities), the result is sensitive to the relation between them (even if they both are vanishingly small!) and, unless a reliable hyperdiffusion model is available, the regularization cannot determine the transition point. This rather unsatisfactory result is quite understandable from the stand point of singular perturbation theory, a category of problem into which the hyperdiffusive regularization falls. As the dependence of such a problem on small parameters is usually nonanalytic [e.g., a boundary layer that behaves as $\exp(-x/\epsilon)$ as $\epsilon\to 0$], the order in which the limits (of the two hyperdiffusivities) are taken clearly matters. Therefore, we also explore methods of determination of the transition point that do not require any additional terms in the transport equations.

It is best to solve an initial value problem. This is difficult in the general case. Thus, with the interest of treatability in mind, we make the plausible assumption that the heat and density relaxation times are significantly different and the heat transport, as the faster process, follows the density transport closely. We develop a variational principle and demonstrate that an underlying functional, akin to a free energy, decreases while the system evolves towards a steady state. Therefore, the correct stationary solution must minimize this functional. We apply this method to the decoupled particle transport equation and again arrive at the Maxwell rule. We can now conclude that the obtained transition loca-

tion within the fueling depth is not caused by a mathematical ambiguity of the governing equations.

To test whether additional terms or physical effects alter this result, we retain the second derivative of the radial plasma pressure profile in the flux suppression term. This automatically increases the order of the system of differential equations, so that the transition point can be located unambiguously. In particular, the transition occurs at a value lower than the Maxwell rule predictions for the heating and particle deposition rate. Since the flux suppression can come from the pressure curvature alone and does not require the density gradient, a striking new result of this approach is the prediction of a pressure gradient driven transition for a flat density profile. In particular, the transition point is no longer located within the fueling depth. Note, that a second derivative term for the density has been included in the nonlinear particle flux of a one-field bifurcation model in Ref. 22. This prediction has implications for the dynamics of pedestal expansion, as we will show.

The remainder of this paper is organized as follows: In Sec. II, the basic transport model is described. A simple substitution is then used to decouple the density and pressure equations. An exact criterion for a stationary state of phase coexistence is obtained. In Sec. III a time dependent variational approach along with a hyperdiffusive regularization are used to determine the exact transition point between the H and L modes in their coexistence range. In Sec. IV we include the curvature of the pressure profile as an alternative regularization for the transition problem. The profile curvature results in a different transition rule than the above two types of regularization. Therefore, in Sec. IV we also study the combined effects of hyperconductivity regularization and profile curvature on the transition rule. In Sec. V we discuss possible time dependent scenarios and hysteresis. This is followed by the discussion and conclusion in Sec. VI.

II. BISTABLE PARTICLE AND ENERGY TRANSPORT MODEL AND ITS STATIONARY SOLUTIONS

In this section we present and simplify the transport model suggested by Hinton and Staebler.[11] This model consists of two coupled diffusion equations for particle and energy transport, including independent particle and heat sources. The particle and heat fluxes are diffusive (with turbulent diffusion) and contain model transport suppression factors related to the effect of the sheared $\mathbf{E}\times\mathbf{B}$ flow. The $\mathbf{E}\times\mathbf{B}$ flow shear is then related to the density and pressure gradients by the radial force balance equation

$$V_E' \simeq \frac{c}{eB}\frac{\partial}{\partial x}n^{-1}(x)\frac{\partial}{\partial x}p(x). \tag{1}$$

The effects of toroidal and poloidal mass flows are neglected. In this model, bistability originates from the multiplicative factor dependent on flow shear. For convenience, we assume slab geometry. Thus, the transport equations can be written as

$$\frac{\partial n}{\partial t} - \frac{\partial}{\partial x}\left[D_0 + \frac{D_1}{1+\alpha V_E'^2}\right]\frac{\partial n}{\partial x} = S(x), \tag{2}$$

$$\frac{3}{2}\frac{\partial p}{\partial t} - \frac{\partial}{\partial x}\left[\chi_0 + \frac{\chi_1}{1+\alpha V_E'^2}\right]\frac{\partial p}{\partial x} = H(x) \tag{3}$$

with V_E' given by Eq. (1). Both the neoclassical transport coefficients (D_0 and χ_0) and the turbulent transport coefficients (D_1 and χ_1) may, in principle, vary with radius x. The constant α parametrizes the level of $\mathbf{E}\times\mathbf{B}$ velocity shear necessary for turbulence suppression. α is obviously related to the turbulence correlation time, $\alpha\sim\tau_c^2$. Here $S(x,t)$ is the particle source and $H(x,t)$ is the thermal source term. In the case of time dependent S and H, they represent the rate of gas puffing and heating power ramps, respectively. Since we are concerned with edge barriers with (standard) edge fueling, $S(x)$ is taken to be localized near $x\simeq a$, while $H(x)$ is localized near $x=0$. Note that it is the flow shear V_E', via its dependence on density and pressure, which couples the two bistable transport equations.

Equations (2) and (3) can be simplified as follows. First, we write

$$g_1 = -\frac{\partial n}{\partial x}, \tag{4}$$

$$g_2 = -\frac{\partial p}{\partial x}. \tag{5}$$

Thus, for stationary n and p, the balance of transport and sources immediately gives the stationarity conditions

$$D_0 g_1 + \frac{D_1 g_1}{1+\alpha V_E'^2} = \int_0^x S(x)dx \equiv \Gamma_s(x), \tag{6}$$

$$\chi_0 g_2 + \frac{\chi_1 g_2}{1+\alpha V_E'^2} = \int_0^x H(x)dx \equiv Q_s(x). \tag{7}$$

Here $\Gamma_s(x)$ and $Q_s(x)$ are the sources balancing the particle and thermal fluxes. For edge barriers, $H(x)$ may be assumed to be peaked at the origin, so that Q_s is constant in the barrier region. However, the spatial dependence of $\Gamma_s(x)$ is important, since $S(x)$ grows sharply towards the edge. Therefore, the formation and structure of edge barriers is indeed sensitive to the fueling profile $S(x)$ [via $\Gamma_s(x)$], but depends only parametrically on the spatially constant heat flux Q_s. One of the gradients, e.g., g_2 can be eliminated by multiplying Eq. (6) by $\chi_1 g_2$, multiplying Eq. (7) by $g_1 D_1$, and then subtracting the results. This yields

$$g_2 = \frac{Q_s D_1 g_1}{\chi_1\Gamma_s - (D_0\chi_1 - \chi_0 D_1)g_1}. \tag{8}$$

Note Eq. (8) allows us to completely decouple Eq. (2) from Eq. (3). Introducing a new variable $g=\alpha^{1/4}\sqrt{cQ_sD_1/eBn^2\chi_1\Gamma_s(x)}g_1$, and substituting Eqs. (1) and (8) into Eq. (6), the latter can be rewritten as

$$F(g) \equiv g + \frac{\lambda g}{1+g^4(1+\Theta g)^{-2}} = \hat{\Gamma}, \tag{9}$$

where

$$\Theta = K^{-1}\sqrt{\chi_1 D_1/Q_s\Gamma_s(x)}(\chi_0/\chi_1 - D_0/D_1), \quad \lambda = D_1/D_0;$$

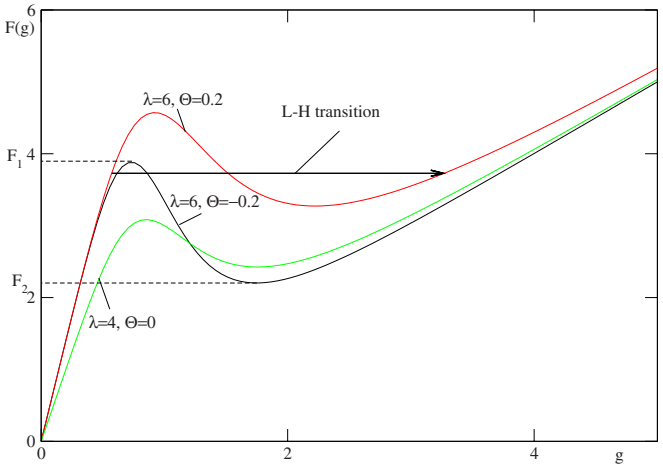

FIG. 3. (Color online) Bifurcation diagram given by Eq. (9) for $\lambda=6$ and different values of parameter Θ. An L→H transition is shown by an arrow.

$$\hat{\Gamma} = KD_0^{-1}\sqrt{Q_s\Gamma_s(x)D_1/\chi_1};$$

and

$$K = \alpha^{1/4}\sqrt{c/eB}n^{-1}.$$

Now, to understand the structure of solutions and bifurcations in the solution $g=g(\hat{\Gamma},\lambda,\Theta)$ it is useful to plot $F(g)$, Fig. 3. First of all, we note that our treatment is limited to a local approximation in the following sense. The function $F(g)$ in Eq. (9) depends not only on the density gradient g but also on the density, temperature and on coordinate x through the parameters involved in Eq. (9). Within the local approximation these quantities are assumed to be fixed at their values at the transition point in $F(g)$. Clearly, the approximation is strictly valid in a small vicinity of the transition point and may become inaccurate far away from it. Also, in Eq. (9), the contribution of the second derivative of the pressure in the flow shear given by Eq. (1) is neglected. This restriction will be relaxed in Sec. IV.

Obviously, a local bifurcation [i.e., an abrupt transition from a smaller to a larger gradient at some radius x, which enters $\hat{\Gamma}(x)$] can occur if Eq. (9) has more than one solution. This requires $F(g)$ to be nonmonotonic, or in other words, an adjacent local maximum and a local minimum should be present. In the simplest case of $\Theta=0$ (which has been studied numerically in Ref. 11) this is only possible if $\lambda=D_1/D_0>\lambda_{\text{crit}}=16/9$. Obviously, L and H modes can coexist where $\hat{\Gamma}(x)$ is between the local minimum and local maximum of $F(g)$. The latter condition can be written in the following symmetric form:

$$\Pi_+ < K\sqrt{\frac{Q_s\Gamma_s}{\chi_0 D_0}} < \Pi_-, \tag{10}$$

where

$$\Pi_\pm \equiv y_\pm^{1/4}\frac{1+\lambda+y_\pm}{1+y_\pm}$$

with

$$y_\pm = \frac{3\lambda}{2} - 1 \pm \frac{3}{2}\sqrt{\lambda\left(\lambda - \frac{16}{9}\right)}.$$

Note that the dimensionless parameters $\Pi_\pm$ depend only on the ratio of transport coefficients $\lambda=D_1/D_0$, which, in this particular case, is equal to χ_1/χ_0, and are thus independent of fueling and heating. The parameter bounded by Π_+ and Π_- in Eq. (10) characterizes power input and fueling in a symmetric way and is related to the corresponding neoclassical transport coefficients.

Evidently, in those regions where $\sqrt{Q_s\Gamma_s/\chi_0 D_0}<\Pi_+/K$, only the L-mode is possible while for $\sqrt{Q_s\Gamma_s/\chi_0 D_0}>\Pi_-/K$, only the H-mode can exist. As we pointed out earlier, Q_s is nearly constant at the transition point while Γ_s changes rapidly with x. Therefore, it is the $\Gamma_s(x)$ profile that determines the pedestal width. However, if the transport coefficients also change on the same scale as Γ_s, then the width of the pedestal may be significantly affected, as seen from Eq. (10).

Equation (10) gives the criterion for the possibility of the local bifurcation in the density gradient at a radius x, for given $Q_s\Gamma_s/\chi_0 D_0$ and $\lambda=D_1/D_0$. Note that Eq. (10) establishes upper and lower bounds on the product $Q_s\Gamma_s(x)$, related to heating and fueling sources, in terms of particle diffusivities and thermal conduction coefficients in L and H modes. This criterion applies to the pressure gradient by virtue of Eq. (8). Equation (10) may be looked at as a criterion for the coexistence of L and H phases. When the product $Q_s\Gamma_s$ is within the range prescribed by this inequality, either mode is consistent with the steady state equations (6) and (7). Equation (10) constitutes a necessary, but not sufficient, condition for L→H bifurcation. Furthermore, it is a local criterion for a bifurcation at a particular point. As long as the exact transition point is not determined, it does not constitute a criterion for, say, the emergence of a density pedestal of a typical width, which is the criterion of practical interest. Finally, note that Eq. (10) states that, in general, a density pedestal requires both particle and heat sources in order to form.

If, as usual, the proportionality between the transport coefficients given by the condition $\Theta=0$ is not fulfilled, the bifurcation problem given by Eq. (9) must be treated in a two-dimensional (λ,Θ) parameter space and its complete study is more tedious. However, another simple result can be obtained in the case of very large $\Theta\gg 1$, in which we easily find the following necessary condition of transport bifurcation $\lambda>\lambda_{\text{crit}}=8$, which is considerably more stringent than that in the case $\Theta=0$. Complete calculations of the steady state bifurcation problem for arbitrary coefficients $\chi_{1,2}$ and $D_{1,2}$ can be more conveniently represented in terms of the following two symmetric combinations of the transport parameters (details are given in the Appendix):

$$A = \frac{D_0}{D_1} + \frac{\chi_0}{\chi_1}; \quad B = \frac{D_0\chi_0}{D_1\chi_1}. \tag{11}$$

The condition for the local bifurcation takes the following form:

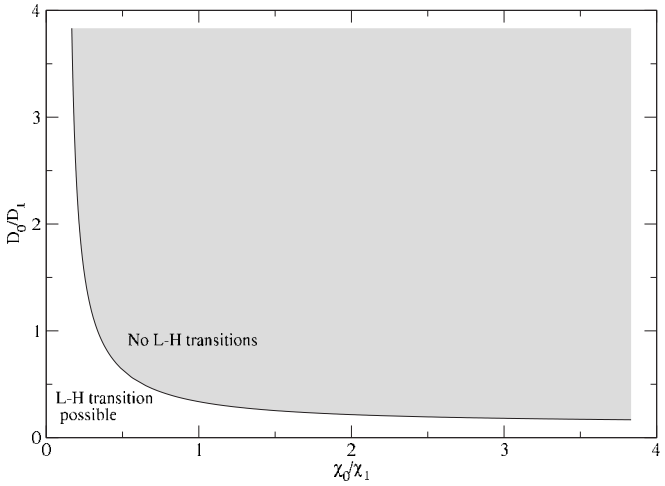

FIG. 4. L–H mode coexistence region in χ_0/χ_1, D_0/D_1 parameter space. In the shaded area no bifurcations are permitted.

$$A^3(32B-4)-4A^4-9A^2+108B(4B-1)<0 \tag{12}$$

which is represented graphically in Fig. 4 as a function of the ratios of transport coefficients D_0/D_1 and χ_0/χ_1. Clearly, strong imbalance of the turbulent components (amenable to shear suppression) relative to the neoclassical ones increases the phase contrast. The resulting magnitude of the gradient jump remains to be determined (see the next section) by obtaining the exact position of the transition within the mode coexistence domain. Nevertheless, at this point we can characterize the "strength" of the transition as a ratio of the local maximum to the local minimum value on the bifurcation curve. This quantity is represented in Fig. 5 and some of the details of its calculation are presented in the Appendix.

III. BIFURCATION THEORY

As we have seen in the previous section Eqs. (6) and (7), or equivalently, Eq. (9) can be satisfied by a family of stationary solutions with different locations of L→H transition. It is important to understand that these equations alone do not uniquely specify the point of transition, just the region of phase coexistence. The reason is that Eq. (9) can be satisfied identically even though g jumps between two different branches of the bifurcation diagram, Fig. 1. Such a jump without variation of $F(g)$ is possible anywhere within the interval given by Eqs. (10) and (A4), i.e., where more than one (in fact three) stationary solution(s) is (are) possible. One possible approach to resolve this uncertainty is to regularize the equation by adding a higher order diffusion term, such as hyperdiffusion.

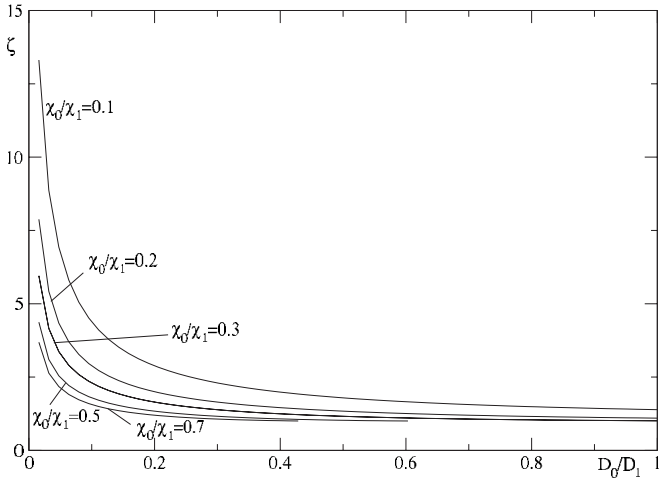

FIG. 5. Bifurcation depth as a function of transport coefficient as given by Eq. (A5).

Such an approach was pursued in Ref. 8 where a flux driven bifurcation [$\Gamma_s(x)\equiv 0$ in, e.g., Eq. (6)] was studied. The transition rule was found to be the ubiquitous equal area (Maxwell) construction. We demonstrate in Sec. III B that the same rule applies to any bistable flux of the type given by Eq. (9), regardless of the specific functional form of flux suppression, so long as the flux is regularized with a second derivative term. Unfortunately, this does not guarantee that the solution of the original time dependent system converges time asymptotically to the same stationary solution selected by the Maxwell rule. Indeed, as we discussed in the Introduction, a consistent regularization would require an addition of regularizing terms to *each* of the stationary equations (6) and (7)[21] and the transition point will depend on their ratio, no matter how small they are. Not only is this ratio unknown, but so are the correct forms of the regularizing terms, as well. Therefore, we must rely on the full time dependent treatment of the original equations, Eqs. (2) and (3). In this treatment, however, we remain in the frame work of weak solutions, i.e., we admit discontinuous gradients of n and p.

It is important to make the following two remarks here. First, the Maxwell construction rule or any other rule for a stationary transition gives a criterion for stationarity of the transition front, not the total disappearance of a phase. Indeed, it seems clear that front stationarity is the relevant criterion for a local transition since the transition will continue while one phase advances into the other. At each point, the Maxwell construction rule specifies the source $\hat{\Gamma}(x)$ strength required for transition front stationarity at that point x. Moreover, front stationarity is a weaker criterion than is disappearance of the L-phase, in that it requires a lower level of driving flux $\hat{\Gamma}$.

A. Time dependent variational approach

To obtain mathematically accurate results in the time dependent case, we assume that the temperature relaxation time is significantly shorter than that of the density, i.e., $\chi_{0,1}\gg D_{0,1}$. Note that in reality, only the first inequality can be considered as marginally valid, while $\chi_1\gtrsim D_1$. Nevertheless, one can make progress by working in the regime where $\chi_{0,1}\gg D_{0,1}$ and then later relaxing the inequality between χ_1 and D_1 somewhat. Now, we can assume that the pressure follows the density quasi-instantaneously (is slaved to it) so one can determine p from Eq. (7) for any moment of time by considering n to be a slow function of time. Formally, the same result can be obtained by a proper ordering of time dependent equations (2) and (3) in the limit $D/\chi\to 0$. Thus,

we express g_2 through g_1 from Eq. (7) and substitute the result into Eq. (2). In fact, it is convenient to express the common suppression factor

$$\frac{1}{1+\alpha V_E'^2} = \frac{1}{1+(K^2 g_1 g_2)^2}$$

through g_2 and substitute this factor into Eq. (2). After differentiating the result by x, and omitting the index at g_1 for brevity, we obtain

$$\frac{\partial g}{\partial t} = \frac{\partial^2}{\partial x^2}\{D_1[\Delta + \omega^{-1}\psi(g)]g - \Gamma_s\}, \tag{13}$$

where $\Delta = D_0/D_1 - \chi_0/\chi_1$, $\omega = \chi_1/Q_s$, and ψ is a branch of $\psi(g)$ fixed by the condition $1<\psi<1+\omega$ and determined by the following relation:

$$g^2 = \frac{\psi^2}{K^4}\frac{\omega+1-\psi}{\psi-1}. \tag{14}$$

In fact, we simply denoted $\psi = 1/g_2$, and we do not need the explicit expression for $\psi(g)$.

Let us now apply a variational approach to the determination of the transition point between the L and H regions when the solution of Eq. (13) approaches the steady state. In contrast to the hyperdiffusion regularization considered in Sec. III B, the variational approach does not require any specific additional terms in Eq. (6), and is therefore more general. We begin with reformulating Eq. (13) in terms of the following variational problem:

$$\frac{\partial g}{\partial t} = \frac{\partial^2}{\partial x^2}\frac{\delta \Lambda}{\delta g}, \tag{15}$$

where the effective "free energy" is given by the following functional:

$$\Lambda = \int_0^a [\Phi(g) - \Gamma_s g]dx \tag{16}$$

and $\Phi(g)$ is defined by

$$\frac{\partial \Phi}{\partial g} = D_1[\Delta + \omega^{-1}\psi(g)]g. \tag{17}$$

Note that Eq. (15) resembles the Cahn–Hilliard equation,[9] except it has a more general functional form of the flux on its r.h.s. In fact, the specific form of the flux Φ' is unimportant so long as it is nonmonotonic. Recall that the steady state solution of Eqs. (15) and (13) is given by

$$\frac{\delta \Lambda}{\delta g} = \Phi'(g) - \Gamma_s(x) = 0, \tag{18}$$

i.e., the functional Λ assumes its extremal value for a stationary solution. As we discussed earlier, the region involved in the transition phenomenon is the one where $\Phi'(g)$ is nonmonotonic, i.e., where $\Gamma_1 < \Phi' < \Gamma_2$. Therefore, to isolate the transition phenomena from the possible influence of the boundaries we assume that $\Gamma_s(a) > \Gamma_2$, i.e., only the H-mode solution is possible and actually realized as a stationary solution, at least in some small vicinity of the right boundary. On the left boundary ($x=0$) we assume that the L-mode solution is established, since there is no fueling in the core. Multiplying Eq. (15) by $\delta\Lambda/\delta g$, integrating it between the boundaries and using the above conditions at the boundaries, along with Eqs. (15) and (16), we obtain

$$\frac{d\Lambda}{dt} = -\int_0^a \left\{\frac{\partial}{\partial x}[\Phi'(g) - \Gamma_s]\right\}^2 dx \leqslant 0. \tag{19}$$

The boundary conditions discussed above also allows us to expand the function $\Phi'(g) - \Gamma_s(x)$ in a series of functions $\sin(\pi n x/a)$ so that we can further refine the last result to

$$\frac{d\Lambda}{dt} \leqslant -\frac{\pi^2}{a^2}\|\Phi'(g) - \Gamma_s\|^2.$$

Here,

$$\|\Phi'(g) - \Gamma_s\|^2 = \int_0^a |\Phi'(g) - \Gamma_s|^2 dx.$$

During the evolution to a steady state, the functional Λ is thus decreasing and

$$\frac{d\Lambda}{dt} = 0$$

only when a steady state solution is reached. In a situation close to a steady state, the functional Λ can be defined on a discontinuous function $g(x)$ which assumes the upper branch values $g = g_+(x)$ for $x > b$ (H-mode) and $g = g_-(x)$ for $x < b$ (L-mode). Here $g_\pm$ are the upper and the lower branches of the solution of Eq. (18), respectively, and $x=b$ is the transition point. Therefore, we can represent Λ as

$$\Lambda = \int_0^b [\Phi(g_-) - \Gamma_s g_-]dx + \int_b^a [\Phi(g_+) - \Gamma_s g_+]dx. \tag{20}$$

Thus, the functional Λ depends both on g and b [or equivalently, on $\Gamma_b = \Gamma_s(b)$]. It can reach its local minimum as a functional of g when b is within the coexistence region. Then, the extremal condition given by Eq. (18) is satisfied. However, this is only a condition for a local minimum of the functional $\Lambda(g;b)$. The global minimum requires in addition

$$\frac{\partial \Lambda}{\partial b} = 0.$$

Substituting Λ from Eq. (20) into the last condition we obtain

$$\Phi[g_-(b)] - \Gamma_b g_-(b) = \Phi[g_+(b)] - \Gamma_b g_+(b). \tag{21}$$

This can also be represented in the form of a "standard" Maxwell rule as

$$\int_{g_-(b)}^{g_+(b)} [\Phi'(g) - \Gamma_b]dg = 0. \tag{22}$$

A further insight into the steady state solution can be gained by considering the density of the functional Λ, i.e., $\Phi(g) - \Gamma g$ which is shown in Fig. 6 as a function of g for three representative values of Γ [Figs. 6(a)–6(c), respectively]. Note that the left local minimum corresponds to the L-mode while the right one corresponds to the H-mode. Evidently, to en-

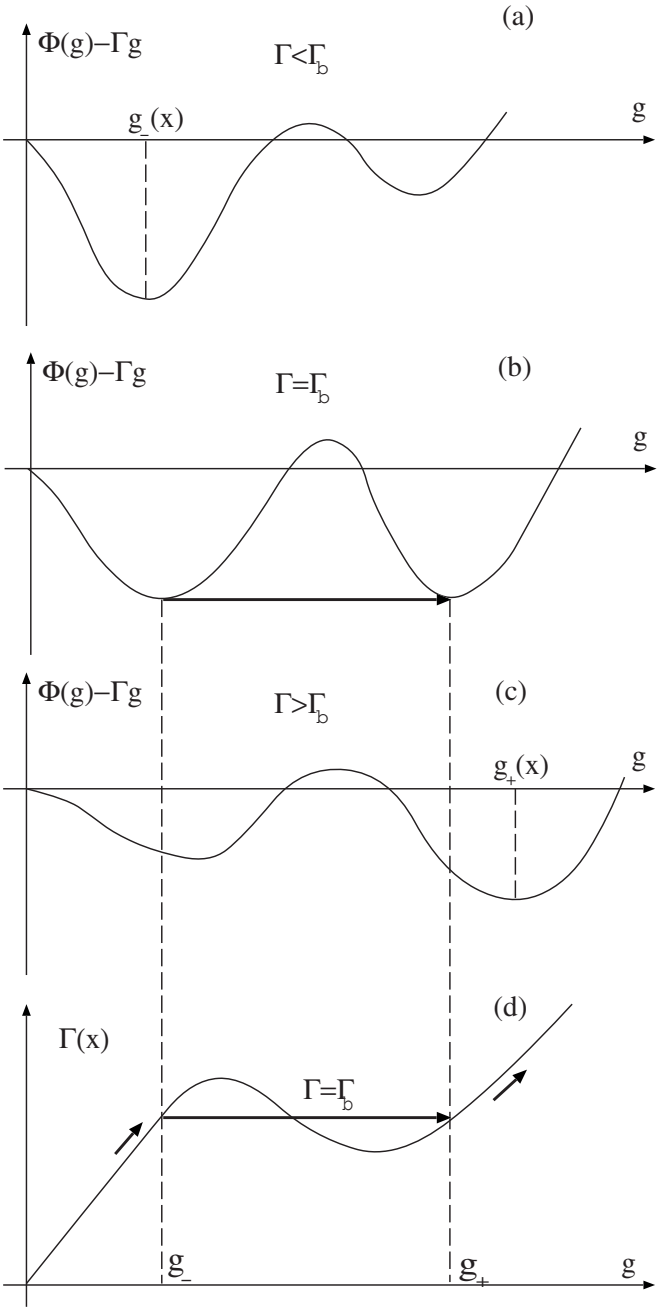

FIG. 6. Three types of behavior of the functional density $\Phi-\Gamma g$ in Eq. (16) and the solution of $g(x)$ that minimizes the functional Λ: (a) the L-mode part of the solution, (b) the L–H transition, and (c) the H-mode solution. The $g-\Gamma$ diagram on (d) shows the Maxwell construction corresponding to the L–H transition in (b).

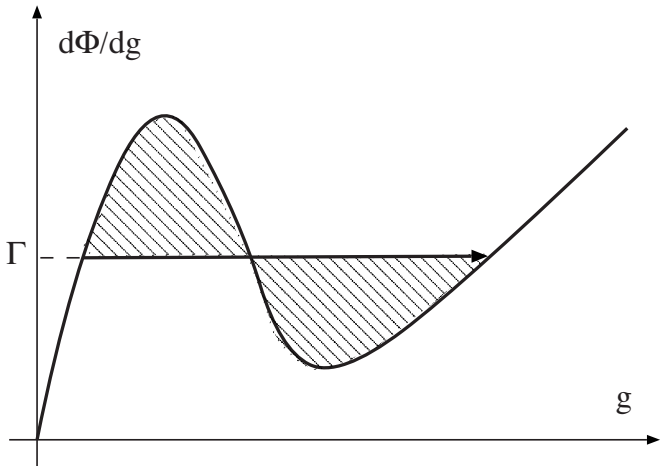

FIG. 7. Depiction of the Maxwell rule for the selection of transition point given analytically by Eq. (16).

sure the global minimum of Λ, $g(x)$ must always follow the lowest of the two local minima of this function, as x varies from 0 to a. Therefore, the transition between the two should occur when they are equal, which is exactly the Maxwell rule transition given by Eq. (21).

Equation (22) is simply the Maxwell construction equal area rule, familiar from the theory of first order phase transitions, Ref. 6. This equation states that the points g_- and g_+ on the bifurcation diagram should be chosen in such a way that the areas above and below the curve of $\partial\Phi/\partial g$, when cut by the line $\Gamma_s=\Gamma_b$, are equal (see Fig. 7). This condition uniquely determines the location of the transition front. However, note that we have now shown this rule to characterize the two-field problem. It is also important to keep in mind that this stationary solution is a special, "weak" solution (with a discontinuous derivative) selected out of a continuum of solutions labeled by the coordinate of the phase transition. The selection principle is based on the time dependent relaxation. Once the time asymptotic limit is reached, the omitted higher derivative terms, even negligibly small in the smooth parts of the solution, become important at the phase transition point and will likely lead to a slow front propagation towards a different stationary position. Clearly, the outcome of such evolution will depend on the dominant higher derivative term included. Therefore, in the next subsection and in Sec. IV we explore regularization approaches that are based on hyperdiffusion and on the curvature of the pressure profile.

B. Hyperdiffusion regularization

With a hyperdiffusive regularization, the steady state problem, given by Eq. (18) becomes

$$\Phi'(g)-\Gamma_s(x)-\varepsilon^2\frac{\partial^2 g}{\partial x^2}=0, \tag{23}$$

where $\varepsilon>0$ is a small parameter. Recall that the one-field problem given by Eq. (18) was obtained from the two-field problem, Eqs. (6) and (7) by eliminating the pressure gradient in favor of the density gradient. Therefore, the regularization in Eq. (23) is equivalent to a special type of regularization of the two-field problem in which hyperdiffusivity pertains only to the particle but not the heat transfer. Here we refer the reader to our earlier discussion of the two-field regularization, given in the Introduction. Returning to Eq. (23) we note that it represents a simple singular perturbation problem ($\varepsilon\to 0$). Introducing an "inner" variable

$$\xi = \frac{x-b}{\varepsilon},$$

where b is the transition front coordinate, to the leading order in $\varepsilon \to 0$ we have

$$\frac{\partial^2 g}{\partial \xi^2} - \Phi'(g) + \Gamma_b = 0. \tag{24}$$

Here the dependence of function Φ on x should be regarded as dependence on a parameter $x=b$ and $\Gamma_b \equiv \Gamma_s(b)$. The solution of this equation (which is the inner solution of the problem) must tend to the discontinuous outer solution as $\xi \to \pm\infty$. These are represented by the H and L roots of Eq. (23) with $\varepsilon=0$. Recall that here discontinuous refers to the fact that the L and H profiles have different slopes. In other words,

$$\lim_{\xi \to \pm\infty} g(\xi, x) = g_{\pm}(x), \tag{25}$$

where $g_{\pm}$ on the r.h.s. are the upper and lower branches of the discontinuous solution of the problem for $\varepsilon=0$. This asymptotic matching condition determines b. Now we consider the first integral of Eq. (24). Multiplying Eq. (24) by $\partial g/\partial \xi$ and integrating yields

$$\int_{-\infty}^{+\infty} d\xi \left[\frac{1}{2} \frac{\partial}{\partial \xi} \left(\frac{\partial g}{\partial \xi} \right)^2 - \frac{\partial g}{\partial \xi} \left(\frac{\partial \Phi}{\partial g} - \Gamma_b \right) \right] = 0.$$

Integrating the first term directly and changing variables to an integration over g in the latter two then yields

$$\frac{1}{2} \left(\frac{\partial g}{\partial \xi} \right)^2 \Bigg|_{-\infty}^{+\infty} - \int_{g_-}^{g_+} \left(\frac{\partial \Phi}{\partial g} - \Gamma_b \right) dg = 0.$$

Since $g \to g_{\pm} = \text{const}$ as $\xi \to \pm\infty$, this result is thus equivalent to

$$\int_{g_-}^{g_+} \left[\frac{\partial \Phi}{\partial g} - \Gamma_b \right] dg = 0. \tag{26}$$

Observe that $g_{\pm} = g_{\pm}(b)$. This is equivalent to the Maxwell rule given by Eq. (22). Strictly speaking, the equivalence of the transition rules in time-dependent and hyperdiffusive case is established in a situation in which hyperdiffusion is added to the density transport (in a steady state) and where we assume that the temperature relaxation is faster than the density relaxation. The equivalence follows from the fact that the description of the temperature relaxation does not require any regularization, due to its rapid rate.

IV. FRONT TRANSITION IN THE PRESENCE OF PRESSURE CURVATURE

A significant simplification in the reduced transport model represented by Eq. (9) has been achieved by neglecting the second derivative of the plasma pressure in Eq. (1). At the same time this makes the steady solution more difficult to obtain, since the relevant equation [Eq. (9)] is algebraic with respect to the pressure gradient and the selection of the correct branch of the solution requires a time dependent treatment, or an *ad hoc* hyperdiffusion regularization. At the same time, retaining the second derivative of the pressure in Eq. (1) preserves the differential character of the transition equation, Eq. (9). Note, that within a one-field model the density curvature effects have been considered in Ref. 22.

Returning to the two field model studied in this paper, and given by Eqs. (2) and (3), from Eq. (1) we obtain

$$\frac{\partial V_E}{\partial x} \simeq -\frac{c}{eBn^2} \frac{\partial n}{\partial x} \frac{\partial p}{\partial x} + \frac{c}{eBn} \frac{\partial^2 p}{\partial x^2}. \tag{27}$$

Observe that since both density and pressure gradients are negative, the first term in the last formula is also negative. So is the last term, since the pressure profile is convex in the L→H transition region. This enhances the flux suppression effect in Eqs. (2) and (3). Moreover, the density profile is likely to be flat in the core if no fueling is present there. In this case the pressure curvature term in Eq. (27) is the only thermal flux suppression term.

We note that higher order transport terms may also be important and we consider a combined action of the pressure curvature and hyperdiffusion later in this paper. We start, however, from a simple consideration of a pure curvature effect and turn then to the situation in which both higher order transport and pressure curvature are present.

A. Bifurcation with no density gradient

Using the relation between the density and pressure gradients given by Eq. (8), the system of Eqs. (6) and (7) reduces to

$$F(g_2, \mu) \equiv g_2 + \frac{(\beta-1) g_2}{1 + \left(\dfrac{\sigma g_2^2}{1+\kappa g_2} + \mu \dfrac{dg_2}{dx} \right)^2} = q(x), \tag{28}$$

where $q = Q_s/\chi_0$, $\beta = 1 + \chi_1/\chi_0$, and the remaining notations used here are as follows:

$$\sigma = \sqrt{\alpha} \frac{c}{eBn^2} \frac{\Gamma_s \chi_1}{Q_s D_1}; \quad \kappa = \frac{D_0 \chi_1 - \chi_0 D_1}{D_1 Q_s}; \quad \mu = \sqrt{\alpha} \frac{c}{eBn} \equiv nK^2.$$

We consider here the case $\mu \neq 0$ but small, that is

$$\mu/a \ll \sigma g_2/(1+\kappa g_2). \tag{29}$$

This allows us to treat the coefficients of the equation as constants (on a scale of the L→H transition which is of the order $l \sim \mu$). Furthermore, by the nature of the transition we assume that the gradient g_2 is monotonically increasing with x from its value g_- on the L-branch of the S-curve to g_+ on the H-branch. One can see from Eq. (28) that $g_2(x)$ increases monotonically along the transition layer only if $F(g_2, 0) > q$ (this inequality should be evaluated at $x=b$, the transition point, since μ is small). To fulfill the last inequality, the transition should start at the lowest possible value of the heat function q, as shown in Fig. 8 by a heavy line. This consideration establishes a minimum heating transition rule for the case of the profile curvature driven transition. The rule replaces the Maxwell rule for this case, as will be confirmed in the next subsection using a stability analysis.

We may see from Eq. (28), in the case $\mu=0$, i.e., if pressure curvature is not considered, an L→H transition can

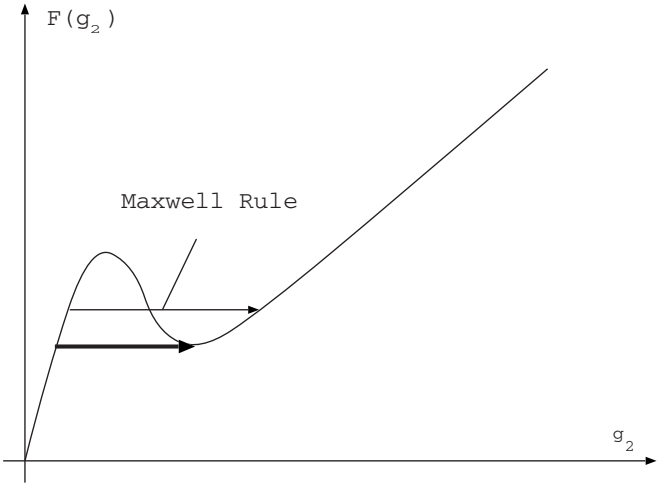

FIG. 8. L→H transition driven by pressure curvature (bottom line) vs Maxwell rule.

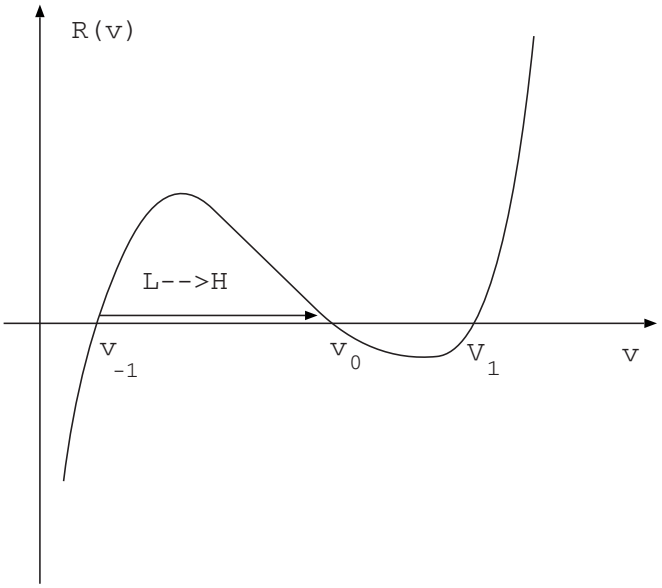

FIG. 9. Depiction of function $R(v)$ in Eq. (31).

only occur when both density and pressure gradients are present (i.e., $\sigma \neq 0$). However, if $\mu > 0$ the situation changes. Let us consider a simple case in which there is no particle deposition in the core, i.e., $\Gamma_s \equiv 0$, so that $g_1 \equiv 0$, or equivalently $\sigma = 0$ in Eq. (28). This equation can be rewritten as

$$\mu \frac{dg_2}{dx} = \sqrt{\frac{\beta g_2 - q}{q - g_2}}. \tag{30}$$

For simplicity we assume that the heat source H in Eq. (3) is constant in some vicinity of the transition point, $H = H_0$. Then, $q(x)$ in Eq. (30) is a linear function coordinate, $q = H_0 x/\chi_0$. Upon substitution $v = \mu g_2/x$, $z = \ln(x/\mu)$, instead of Eq. (30) we obtain

$$\frac{dv}{dz} = \sqrt{\frac{\beta v - h_0}{h_0 - v}} - v \equiv R(v) \tag{31}$$

with $h_0 = \mu H_0/\chi_0$. Depending on the parameters β and h_0 this equation has three or one fixed points, $R(v) = 0$, as shown in Fig. 9. Let us consider the case when the three roots of $R(v)$ are present, and denote them as $v_{-1} < v_0 < v_1$. They can be expressed through the parameters β and h_0 as follows:

$$v_n = \frac{h_0}{3} + \frac{2}{\sqrt{3}}\sqrt{\frac{h_0^2}{3} - \beta}\sin\left\{\frac{2\pi n}{3} - \frac{1}{3}\sin^{-1}\left[\frac{3^{3/2} h_0}{2(h_0^2/3 - \beta)^{3/2}}\left(1 + \frac{2}{27}h_0^2 - \frac{1}{3}\beta\right)\right]\right\}. \tag{32}$$

The smallest root $v = v_{-1}$ corresponds to the L mode solution. This is easy to see for the simple case $1 \ll h_0 \ll \beta \ll h_0^2$ directly from Eq. (31). Indeed, in this case $v_{-1} \approx h_0/\beta$ corresponds to the solution $g_2 = Q_s(x)/(\chi_0 + \chi_1)$, which is clearly an L-mode solution since the turbulent thermoconductivity χ_1 is not suppressed. However, the fixed point v_{-1} is an unstable equilibrium of Eq. (31) [since $R'(v_{-1}) > 0$]. Therefore the system must leave this point and transit to the stable fixed point $v = v_0 \approx \beta/h_0$ as z changes from $z = -\infty$ $(x = 0)$, to $z \to \infty$. Recall that $z = \ln(x/\mu)$ and thus plays the role of an internal variable of the transition, since x is scaled to the small parameter (μ) in the highest derivative term in Eq. (30). Therefore, as z varies between $-\infty$ and $+\infty$, the system transits from the L to H mode. However, both fixed points v_{-1} and v_0 may vanish for a certain range of parameters h_0 and β (see below). The remaining fixed point v_1 is unstable and the system must transit from this point to the singular point of Eq. (31), $v = h_0$. However this solution must be rejected on the ground that it cannot be continued along the z axis beyond a critical point z_0, where it collapses as $(h_0 - v) \propto (z_0 - z)^{2/3}$. We thus conclude that the L→H transition requires the heating rate h_0 to exceed a threshold value which ensures the coexistence of all three roots v_n. The latter requires that the argument of *arcsin* in Eq. (32) falls within the interval $(-1, 1)$.

B. Bifurcation in the presence of thermal hyperconductivity

Since the hyperdiffusion regularization and the pressure curvature lead to different transition rules (Maxwell equal area and minimum heating rate, respectively), in this subsection we study both effects, acting together. Equation (28) generalizes to the following form, where we write g instead of g_2, for short

$$g + \frac{(\beta - 1)g}{1 + (\sigma g^2 + \mu dg/dx)^2} - \varepsilon^2 \frac{d^2 g}{dx^2} = q(x). \tag{33}$$

The notations here are the same as in Eq. (28) while the new length scale ϵ characterizes the hyperconductivity. We assumed for simplicity that $\kappa g_2 \ll 1$. Let us also assume that characteristic scale of the heat source q is $L_q \gg \epsilon$ and μ is a small parameter. Working in the vicinity of the front transition at $x \simeq b$, so that $q \simeq q(b) = \text{const}$ we obtain from the last equation

$$H(g,g_x) \equiv \frac{\varepsilon^2}{2}\left(\frac{dg}{dx}\right)^2 - \frac{1}{2}g^2 + qg - \frac{1}{2\sigma}(\beta-1)\tan^{-1}(\sigma g^2) + \mu(\beta-1)D(g) = H_0, \tag{34}$$

where H_0 is an integration constant. This expression can obviously be interpreted as the energy of a nonlinear oscillator that is described by its coordinate g and velocity $dg/dx \equiv g_x$. The last term is responsible for a weak nonlinear "dissipation" [small μ, cf. Eq. (33)] and the function $D(g)$ is given by the following formula:

$$D = \int \frac{2\sigma g^2 g_x(g) + \mu g_x^2(g)}{(1+\sigma^2 g^4)[1+(\sigma g^2 + \mu g_x)^2]} g dg \tag{35}$$

which can be evaluated by solving Eq. (34) for g_x to zeroth order in μ.

Three critical points of the "Hamiltonian" in Eq. (34) now correspond to the three solutions of the problem discussed above, i.e., without thermal hyperconductivity, Eq. (28). The L→H transition is then represented by a separatrix of the dynamical system given by Eq. (34) (with $\mu=0$) which connects two hyperbolic points. A similar situation has already been considered earlier in Sec. III B. The difference is that the H-level at the two hyperbolic points is different because of the dissipation term in Eq. (34). This produces a deviation from the Maxwell rule which can be calculated as follows.

We start with treating the "dissipation" μ as a small parameter compared to the "inertia" ϵ. The transition rule can be characterized by a magnitude of the heating source q at the transition point which, in turn, can be expanded in a series of μ,

$$q = q_M + \mu q_1 + \cdots.$$

Here q_M is the Maxwell rule value of q already calculated in Sec. III. The L- and H-mode solutions $g_\pm$, as it can be readily seen from Eq. (34), do not depend on μ, since they are the stationary points of the Hamiltonian H and $\partial D(g_\pm)/\partial g = 0$. To simplify the algebra we obtain these solutions by assuming that $\sigma g_-^2 \ll 1$ and $\sigma g_+^2 \gg 1$. The equations for $g_\pm$ are as follows:

$$\frac{\partial}{\partial g} H(g_\pm, 0) = 0,$$

so using the assumptions above, we obtain

$$g_- \simeq q/\beta, \quad g_+ \simeq q \tag{36}$$

so that β must be rather large. The equations for q and the constant H_0 read

$$H(g_-,0) = H(g_+,0) = 0$$

which can be written as

$$\frac{\beta}{2}g_-^2 - qg_- = \frac{1}{2}g_+^2 - qg_+ + \pi\frac{\beta-1}{4\sigma} - 2\mu\sigma(\beta-1) \times \int_{g_-}^{g_+} \frac{g_x(g)g^3}{(1+\sigma g^4)^2} dg$$

while $H_0 \simeq q^2/2\beta$. For q, we thus have

$$q = \sqrt{\frac{\pi\beta}{2\sigma}\left[1 - \frac{8}{\pi}\mu\sigma^2 \int_{g_-}^{g_+} \frac{g_x(g)g^3}{(1+\sigma^2 g^4)^2} dg\right]}.$$

The integral in the last equation can be calculated from Eq. (34) using the above formula for the constant H_0. In the limit $\beta \gg 1$ we finally obtain the following formula for the heating rate at the transition point:

$$q = \sqrt{\frac{\pi\beta}{2\sigma}\left[1 - \frac{4\mu}{\pi\varepsilon}\sqrt{\frac{\beta}{\sigma}}(\ln\beta - 3)\right]}. \tag{37}$$

In the limit $\mu \to 0$ this expression reduces to the case with no curvature effects, i.e., to the Maxwell transition rule established in Secs. III A and III B. The Maxwell rule can be obtained directly from Eq. (28) by writing the equal area requirement in the following form:

$$\int_{g_-}^{g_+} [F(g) - q] dg = 0,$$

where $g_\pm$ are given by Eq. (36). We can see by inspection that the correction to the Maxwell rule associated with the profile curvature in Eq. (37) is very large for large β and small ϵ even if the curvature term (μ) is small. However, $\beta \equiv 1 + \chi_1/\chi_0$ should exceed $e^3 \approx 20$ in order to reduce the power threshold for the transition. Therefore, it seems to be reasonable to suggest that in the presence of the curvature effect, the stationary transition should obey the minimum power rule established in the previous subsection. However, Eq. (37) becomes invalid when the correction term associated with the curvature is not small. Therefore, to confirm this suggestion, we turn to the case of small ϵ, for which from Eq. (33) we have

$$\mu\frac{dg}{dx} = \sqrt{\frac{\beta g - q}{q - g}} - \sigma g^2. \tag{38}$$

In terms of a more general dynamical system described by Eq. (33) the solution of the last equation corresponds to the frictional slide of the trajectory from an unstable equilibrium at $g = g_-$ to the stable one at $g = g_0$, which is an intermediate (between g_- and g_+) root of the r.h.s. of Eq. (38). This is a *stationary* L→H transition solution of the underlying nonlinear diffusion equation supplemented with the pressure curvature term, i.e.,

$$\frac{\partial g}{\partial t} = \frac{\partial^2}{\partial x^2} F(g, g_x), \tag{39}$$

where

$$F(g,g_x) \equiv g + \frac{(\beta-1)g}{1 + (\sigma g^2 + \mu dg/dx)^2} - q(x).$$

However, in the context of this time dependent equation the solution $g = g_0$ is still unstable (at least for sufficiently small μ). The reason for the instability is very simple. The linearization of Eq. (39) about the solution $g = g_0$ leads to an equation with a negative diffusivity since

$$\frac{\partial}{\partial g} F\big|_{g=g_0} < 0$$

and linearized solutions of Eq. (39) are indeed unstable near $g=g_0$. In other words, the underlying bistability remains (only g_- and g_+ branches of the S-curve are stable), despite pressure curvature. On the other hand, we demonstrated that precisely the g_0 solution is an endpoint for the stationary transition. The only way to reconcile the instability of the intermediate solution g_0 and the fact that this solution is the endpoint for the stationary transition is by merging the unstable and stable points g_0 and g_+. This result agrees with the transition rule established in the previous subsection for the case of the profile curvature regularization (with v_0 and v_1 roots being equivalent to g_0 and g_+). This requirement determines the transition point since such merging is only possible at a specific value of the source $q(x_b)$. With q growing beyond $q(x_b)$, the stationary solution proceeds, as always, along the stable $g=g_+$ branch of the S-curve. Then, the actual stationary transition from the L-mode solution g_- to the H-mode solution g_+ in a situation where profile curvature effects dominate the hyperthermoconductivity effects should occur at the minimum of the S-curve [see Fig. 8 and also the discussion following Eq. (29) in the preceding subsection].

V. TIME DEPENDENT SCENARIO, COMPARISON OF DIFFERENT TRANSITION RULES AND HYSTERESIS

In this section we consider possible implications of our results for the temporal evolution of the bifurcation. To establish a theoretical framework for our consideration, we assume that the heating rate Q_s is ramped up slowly (with all other control parameters fixed), so that the quasisteady solutions discussed above are relevant. Let us recast the phase coexistence condition, given by Eq. (10), in the simplest form possible as

$$Q_1 < Q_s < Q_2. \tag{40}$$

As long as $Q_s < Q_1$, the system must clearly be in the L state [lower root of Eq. (9) should be chosen]. When Q exceeds Q_1 (note that this happens first at the edge, since Γ_s is peaked there and $Q_{1,2} \propto 1/\Gamma_s$), the system can jump to the H-mode at some point where $Q_s > Q_1$ but it does not need to jump. When the heating is increased beyond Q_2, the system must be in the H-mode at all points where $Q_s > Q_2$. Now the question is where exactly in the interval $Q_1 < Q_s < Q_2$ does the L to H transition actually occur?

Hinton[10] suggested the following rule (also utilized in Ref. 11). The system must stay at the L branch as long as possible, which implies that the forward transition occurs at $Q_s = Q_2$. On the way back, when Q_s is decreased from its value exceeding Q_2 down to $Q_s < Q_1$, the reverse transition should occur (by the same token) only at $Q_s = Q_1$. This rule clearly implies the strongest hysteresis possible in this system. At the same time, the fact that the reverse bifurcation occurs at $Q_s = Q_1$ ensures that the resulting stationary profile has the smoothest possible form (the smallest jump in g, see the S-curve in, e.g., Fig. 1), a property which apparently was one of the motivations for this rule. Even though only steady state solutions are considered, it is useful to understand how their branches switch when the fueling increases at the wall. So long as $Q_s < Q_2$, the L-mode solution occupies the whole range. Only when Q_s exceeds Q_2, the H-mode phase appears at the domain boundary (separatrix), where Q_s reaches its maximum (because Q_s follows the fueling profile). This is clearly different from the Maxwell rule and even more so from the minimum heating rule, by which the forward transition occurs at the midpoint between Q_1 and Q_2, and at $Q_s = Q_1$, respectively. However, once established at the wall, the H-phase should propagate (as is usual for 0D dynamical systems) to the point $Q_s = Q_1$, formally coinciding thus with the minimum heating rule. The important difference is that the curvature driven transition does not need to be inside the fueling depth and may propagate further as long as the heating requirement is met.

Returning to the 0D rule, we now follow the solution starting from its L-mode side. Obviously, the solution turns out to be in conflict with the declared rule of sticking to the L-branch as long as possible. Indeed, according to this rule the solution should be in the L-mode up to $Q_s = Q_2$. This rule, being perfectly applicable to low-dimensional dynamical systems (where there is no spatial overlap of different branches of the solution) clearly fails in continuous media, since it prescribes different solutions depending on the direction from which the phase coexistence region is approached! This argument pinpoints a major shortcoming in the "conventional wisdom" of the L→H transition.

Our treatment in Secs. III and IV has shown that the transition should obey the Maxwell rule in the case without pressure curvature, and the rule of lowest possible Q_s transition if the curvature effects are retained. Both rules, applied in isolation, preclude hysteresis. One can identify, however, at least two phenomenological reasons to alter this conclusion. The first reason is that more realistic flux suppression mechanisms are probably at least somewhat nonlocal, so that the suppression efficiency should depend on such factors as the pedestal height and width. This may introduce asymmetry into the bifurcation process. Specifically, the forward L→H may change the entire S-curve by lowering the transition thresholds because of the higher core temperature, Fig. 10. Therefore, if the Maxwell rule applies, the reverse bifurcation should occur at lower Q_s, thus leading to hysteresis. The second reason involves the curvature of the pressure profile. In L-mode this effect may be negligible, while after the L→H transition a pedestal, along with a narrow region of significant curvature of the pressure profile, $\partial^2 p(x)/\partial x^2$, both form. Indeed, existence of the pedestal necessitates the region of strong curvature. Therefore, at the reverse H→L transition, curvature must be included. Since, as we have seen, the transition should occur at the lowest possible Q_s, this forms a hysteresis loop with the forward Maxwell transition. In this latter case the depth of the hysteresis is determined and it is approximately half (in the Maxwell sense) of that prescribed by the 0D rule.[10]

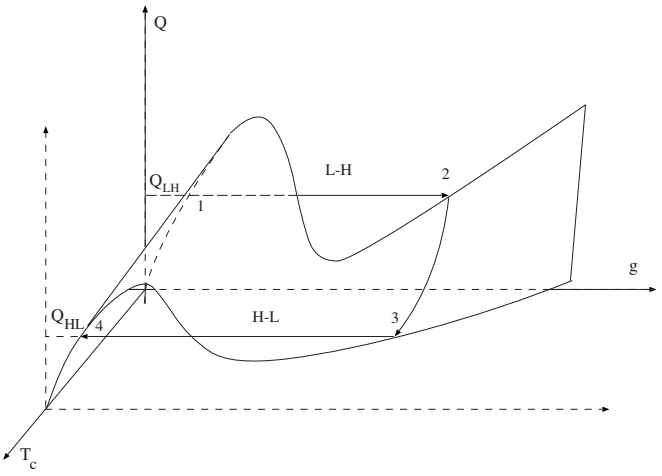

FIG. 10. Hysteresis phenomenon in the L–H transition in a three-dimensional parameter space that also includes the core temperature; first, the L–H transition (1–2) occurs at a relatively low rate since the system starts from the L mode. When the gradient g builds up at the edge, increases (2–3) lowering thus the heating requirements for transitions. Then, if the heating Q decreases to its Maxwell value, the reverse transition occurs at lower Q than the forward one.

VI. CONCLUSIONS AND DISCUSSION

In this paper, the two field bifurcation model is extended to include the pressure curvature, time dependence, and higher order regularization. The model is solved analytically. The principal results of this paper are:

(i) A simple substitution allows decoupling of the density and pressure evolution equations. This decoupling is exact for steady state.

(ii) An analytical criterion for the coexistence of the L-phase and H-phase is derived [Eqs. (10) and (12) and Fig. 4]. The expression in Eq. (10) bounds the required product of local heat and particle fluxes with expressions involving the ratios of heat and particle transport coefficients in L and H mode. These results are considerably more general than those of Ref. 11.

(iii) In the case of negligible curvature of the pressure profile [see (vii) below], the region of coexistence of L and H phases (i.e., the region where a transition may occur, though it need not) is limited by the fueling depth, for central heat deposition. Note, however, that the fueling depth does not by itself determine the pedestal width.

(iv) A local transition criterion is derived. This criterion is based upon satisfying the conditions necessary for the spatial advance of one phase (i.e., L) into the other (i.e., H). We show that the local transition criterion is equivalent to the Maxwell construction rule.

(v) Detailed regularization arguments are given to support the conclusions of (iii)–(iv), above. Two independent approaches are used, one in which a hyperdiffusion is added and one which uses a time dependent variational approach. The results of both these procedures agree on the Maxwell construction rule, which may then be evaluated to obtain the pedestal width. Transport analysis is required to obtain experimentally relevant pedestal width predictions from the Maxwell rule formalism. This will be addressed in future publications.

(vi) The Maxwell rule criterion is shown to preclude local hysteresis. Thus, we argue that hysteresis must necessarily be due to profile effects. Therefore, the space-time evolution of the S-curve must be considered in order to accurately represent hysteresis, or pressure curvature should be included (see below).

(vii) An alternative approach to the regularization problem, which is based on the inclusion of the curvature (second derivative) of the pressure profile, is developed. Inclusion of curvature results in softening the threshold requirements, as compared to the conventional regularization mentioned above. With profile curvature, the transition is shown to be possible even within a region of a flat density profile (i.e., where there is no fueling). Technically, this transition scenario also precludes hysteresis, but if the curvature effects are negligible for the forward transition, they will surely become important for the reverse (H→L) transition (i.e., due to development of pedestal), and hysteresis will be recovered. The strength of the hysteresis amounts to the difference between the Maxwell (L→H) and the minimum heating rate Q_s (minimum of the S-curve). This is roughly half the conventional estimate of the hysteresis.

Several comments are in order here. First, in the spirit of "truth in advertising," we reiterate that the model considered here is simplistic and limited, on account of its "minimalist" approach to the physics of shear suppression of turbulence and its postulate of fixed and spatially constant transport coefficients. Also, the restriction of the theory to "gentle" transitions renders it inapplicable to cases of fast power ramps, etc., and most relevant to slow transitions, which reveal the most about L→H transition dynamics. Second, since the paper raises at least as many questions as it answers, the agenda for future work is indeed a lengthy one. First, the simultaneous regularization of density and pressure (or temperature) evolution must be completed. This, then, would form the foundation for a rigorous solution of the "dual pedestal width" calculation, for density and temperature. Third, this type of calculation must be implemented along with transport analysis (including cross phase shift and decorrelation, observationally confirmed to be important, e.g., Ref. 23). Thus, the unphysical modeling constraints on transport coefficients may be relaxed. Finally, the effects of noise, Ref. 24 and of MHD stability limits, Refs. 19 and 25–29 should be included. The latter is a necessary element of any model of ELM phenomena, Ref. 30. MHD stability may ultimately limit barrier penetration.

The effect of finite curvature of the radial pressure profile studied in this paper appears to be important in both the edge and core of tokamak plasmas. In the case of an edge plasma, where both pressure and density gradients are important for barrier formation, a new rule for the barrier location is established. In contrast to the hyperdiffusion regularization, which results in the Maxwell equal area rule for the

transition (driven by both the boundary flux[8] and by a distributed particle source considered in this paper), in the finite pressure curvature case the transition occurs at the lowest possible value of thermal flux. This implies a weaker power requirement for the H-mode to occur. Moreover, we demonstrated that the pressure gradient transition can occur even with a flat density profile. Therefore, the transition point can be outside the fueling profile, so that the pedestal may be broader than the fueling depth. This observation may potentially explain how the pedestal can extend beyond the fueling depth.

The profile curvature driven L→H transition is thus strikingly different from the standard coupled fluxes model[11] in which the density and pressure barriers are strongly coupled. Note that our formula for the coupling between gradients given by Eq. (8) (which is valid for arbitrary pressure curvature) in the region where no fueling is present ($\Gamma_s=0$) takes an indeterminate form $(0/0)$ and the equation for the pressure gradient g_2 is independent of the density gradient ($g_1=0$) in this case. Obviously, the co-location of the density and pressure transitions which follows from Eq. (8) is no longer the case here.

Since attempts at building a simple model of the transition now mark a well-trodden path, some discussion of the relation of this paper to previous work is appropriate here. We already have made extensive comparison and contrast of our results with these of Ref. 11, this paper's closest antecedent. Hence, no further comments on Ref. 11 are given below. Regarding the ever-popular Waltz "rule,"[31] based on the comparison of the linear growth rate with the local "shearing rate," it seems clear that this approach gives no information about either bifurcation dynamics or H-mode layer widths, and serves only as an indicator of when shearing effects "might" become important. Similarly, heuristic approaches serve only as a test of various *ad hoc* choices for the transition layer scale and have no foundation in fundamental physics or potential for prediction. Indeed, the bistable sandpile model of Gruzinov *et al.*[32] gives an excellent demonstration of the failure of the scaling approach. The empirical model of Groebner *et al.*,[33] which links the H-mode layer or pedestal width directly to the fueling profile (i.e., neutral deposition profile) is oversimplified, in that it downplays *a priori* the effects of heating power and turbulent transport, and offers no physics-based argument as to why the fueling profile should be the primary element in determining the layer scale. Indeed, indications to the contrary are discussed in Ref. 34. The bistable sandpile model of Gruzinov *et al.*[32,35] is also, in essence, a "one-field" model, which does not account for heating power effects, etc. Finally, the interesting "noisy transition" model proposed by Itoh *et al.*[24] is also limited to one field, does not treat heating and fueling, and incorporates additive noise, only. This paper does make the important point that noise-induced fluctuations can enable the transition to "tunnel" through the barrier associated with the Maxwell rule. While incomplete at present, this approach, when expanded to treat multiple fields, transport, and multiplicative noise, could yield very interesting results.

While this paper is decidedly theoretical, it does, however, offer several predictions suitable for study by experimentalists. First, this theory rigorously demonstrates that density and pressure profile development are related, but not identical. In particular, bifurcations of density and pressure may occur at different points, and the structure of density and pressure pedestals may be different. Moreover, both pedestals can be expected to expand with increasing heating power. Pedestal expansion with increasing drive was observed in the studies of Refs. 32 and 35. These predictions are quite amenable to experimental study. Indeed, there already are some indications that this is the case in experiments.[20] Unfortunately, quantitative tests must await the solution of the "dual regularization" problem and the implementation of the theory in concert with transport analysis. Second, the theory predicts that, ignoring profile curvature, the range of possible transition locations (i.e., the phase coexistence region) is set by the fueling depth, assuming central heat deposition. Thus, any departure of the pedestal width from the neutral penetration depth is *prima facie* evidence for the importance of profile curvature effects or other departures from the simple model. Third, the theory predicts that hysteresis is linked to profile structure and is fundamentally nonlocal. This idea naturally suggests studies of the back-transition in the presence of modest or weak gas-puffing, which would alter H-mode density profiles and thus should impact hysteresis. Of course, the aim would be to compare the empirical hysteresis for different H-mode edge density profiles and pedestal widths. Finally, a central result of this paper is that the criterion for advance of the barrier without pressure curvature is given by the Maxwell construction rule even for the two field model. When the pressure curvature is included, the transition occurs at the lowest possible heating rate. A potentially observable consequence of the Maxwell rule and the minimum power rule is the disparity between the pedestal width and the width of the fueling profile. While a quantitative test of this prediction requires transport analysis, the use of slow ramps and transitions, may enable one to empirically construct an S-curve, as was done in Ref. 20, and see if barrier front stationarity coincides with a deposition strength which satisfies Maxwell's rule at the barrier boundary. More generally, it would be interesting to determine a generic Maxwell rule scaling for typical pretransition profiles, edge transport, etc.

ACKNOWLEDGMENTS

We thank many individuals for numerous discussions which greatly stimulated this work; among them are F. Hinton, X. Garbet, P. Ghendrih, A. Hubbard, C. S. Chang, T. S. Hahm, K. H. Burrell, R. J. Groebner, and Y. Sarazin. We are particularly indebted to the late M. N. Rosenbluth for his invaluable insight into the regularization problem and other aspects of this study. P. H. Diamond would like to thank the participants in the Festival de Theorie (supported by C.E.A.) 2005 and 2007 for many stimulating discussions.

This research was supported by the Department of Energy Grant No. DE-FG02-04ER54738.

APPENDIX: DERIVATION OF A GENERAL COEXISTENCE CRITERION

Dividing the steady state transport equations (6) and (7) by D_0 and χ_0, respectively, and then multiplying the results by each other, we arrive at the following equation for only one variable $y=K^4 g_1^2 g_2^2 \geqslant 0$:

$$U(y) \equiv \sqrt{y}\left(1+\frac{D_1/D_0}{1+y}\right)\left(1+\frac{\chi_1/\chi_0}{1+y}\right) = K^2\frac{\Gamma_s Q_s}{D_0\chi_0} \equiv P, \tag{A1}$$

where we have used the following notation: $K^2=\sqrt{\alpha}c/eBn^2$. Note a completely symmetric form of the last equation with respect to the particle and heat components. Clearly the mode coexistence is only possible if the above expression has two local extrema. It is somewhat more convenient to elaborate a condition for the above requirement, if one is using $\ln U$ instead of U and a new variable $t=1/(1+y)$ instead of y. Differentiating then $\ln U$ with respect to t we obtain the following condition for the extrema:

$$\frac{1}{t+D_0/D_1}+\frac{1}{t+\chi_0/\chi_1}-\frac{1}{2t(1-t)}=0. \tag{A2}$$

This leads to a cubic equation which has either one or three real roots. The latter is necessary for the mode coexistence. The condition for the three real roots to exist can be shown to have the form given by Eq. (12). Note that in the special case $D_1/D_0=\chi_1/\chi_0$ considered earlier in Sec. II, the inequality in Eq. (12) reduces to $\chi_1/\chi_0>16/9$. The sufficient condition for the L–H transition, however, is the requirement that the range of the power source P in Eq. (A1) contains the interval $[U_{\min},U_{\max}]$, where the latter two quantities refer to the local minimum and maximum of the function $U(y)$.

Using a new variable $z=t+A/6-1/4$ instead of t in Eq. (A2), we obtain the following cubic equation for the extrema:

$$z^3-3\rho^2 z+\sigma=0, \tag{A3}$$

where we denoted

$$\rho=\frac{1}{12}\sqrt{4A^2+9}$$

and

$$\sigma=\frac{A^3}{108}+\frac{B}{4}-\frac{1}{32}.$$

The condition for the three real roots to exist is $\sigma^2<4\rho^6$, from which we recover Eq. (12). The two roots of interest are

$$z_{\min}=-\rho\cos\phi+\sqrt{3}\rho\sin\phi$$

and

$$z_{\max}=2\rho\cos\phi$$

which correspond to the local minimum and local maximum of $U(z)$ in Eq. (A1), i.e., $U_{\min/\max}=U(z_{\min/\max})$. We denoted

$$\phi=\frac{\pi}{3}-\frac{1}{3}\cos^{-1}\left(\frac{\sigma}{2\rho^3}\right).$$

The mode coexistence region is thus given by the following inequality:

$$U_{\min}<K^2\frac{\Gamma_s Q_s}{D_0\chi_0}<U_{\max}. \tag{A4}$$

The "depth" of the bifurcation can thus be defined as

$$\zeta\equiv\frac{U_{\max}}{U_{\min}}=\left[\frac{A/6+3/4-2\rho\cos\phi}{A/6+3/4+2\rho\cos(\phi+\pi/3)}\right]^{3/2}\times\left[\frac{1/4-A/6+2\rho\cos\phi}{1/4-A/6-2\rho\cos(\phi+\pi/3)}\right]^{1/2}\times\frac{A/3+1/4+2\rho\cos\phi}{A/3+1/4-2\rho\cos(\phi+\pi/3)}. \tag{A5}$$

This quantity is plotted in Fig. 5 for different values of transport coefficients.

[1] F. Wagner, G. Becker, K. Behringer, D. Campbell, A. Eberhagen, W. Engelhardt, G. Fussmann, O. Gehre, J. Gernhardt, C. v. Gierke, G. Haas, M. Huang, F. Karger, M. Keilhacker, O. Klüber, M. Kornherr, K. Lackner, G. Lisitano, G. G. Lister, H. M. Mayer, D. Meisel, E. R. Müller, H. Murmann, H. Niedermeyer, W. Poschenrieder, H. Rapp, H. Röhr, F. Schneider, G. Siller, E. Speth, A. Stäbler, K. H. Steuer, G. Venus, O. Vollmer, and Z. Yü, Phys. Rev. Lett. **49**, 1408 (1982).
[2] Y. Koide, M. Kikuchi, M. Mori, S. Tsuji, S. Ishida, N. Asakura, Y. Kamada, T. Nishitani, Y. Kawano, T. Hatae, T. Fujita, T. Fukuda, A. Sakasai, T. Kondoh, R. Yoshino, and Y. Neyatani, Phys. Rev. Lett. **72**, 3662 (1994).
[3] S. I. Itoh and K. Itoh, Phys. Rev. Lett. **60**, 2276 (1988).
[4] H. Biglari, P. H. Diamond, and P. W. Terry, Phys. Fluids B **2**, 1 (1990); T. S. Hahm and K. H. Burrell, Phys. Plasmas **2**, 1648 (1995).
[5] K. H. Burrell, Phys. Plasmas **4**, 1499 (1997).
[6] E. M. Lifshitz and L. P. Pitaevski, *Statistical Physics, Part I* (Pergamon, Oxford, 1980).
[7] P. H. Diamond, Y.-M. Liang, B. A. Carreras, and P. W. Terry, Phys. Rev. Lett. **72**, 2565 (1994).
[8] V. B. Lebedev and P. H. Diamond, Phys. Plasmas **4**, 1087 (1997).
[9] J. W. Cahn, Trans. Metall. Soc. AIME **242**, 166 (1968).
[10] F. L. Hinton, Phys. Fluids B **3**, 696 (1991).
[11] F. L. Hinton and G. M. Staebler, Phys. Fluids B **5**, 1281 (1993).
[12] G. M. Staebler, F. L. Hinton, and J. C. Wiley, Plasma Phys. Controlled Fusion **38**, 1461 (1996).
[13] ASDEX Team, Nucl. Fusion **29**, 1959 (1989).
[14] P. H. Diamond, V. B. Lebedev, D. E. Newman, B. A. Carreras, T. S. Hahm, W. M. Tang, G. Rewoldt, and K. Avinash, Phys. Rev. Lett. **78**, 1472 (1997).
[15] L. Chen, Z. Lin, and R. White, Phys. Plasmas **7**, 3129 (2000).
[16] M. A. Malkov, P. H. Diamond, and M. N. Rosenbluth, Phys. Plasmas **8**, 5073 (2001).
[17] E. Kim and P. H. Diamond, Phys. Plasmas **9**, 4530 (2002).
[18] P. H. Diamond, V. B. Lebedev, Y. M. Liang, A. V. Gruzinov, I. Gruzinova, M. Medvedev, B. A. Carreras, D. E. Newman, L. Charlton, K. L. Sidikiman, D. B. Batchelor, E. F. Jaeger, C. Y. Wang, G. G. Craddock, N. Mattor, T. S. Hahm, M. Ono, B. LeBlanc, H. Biglari, F. Y. Gang, and D. J. Sigmar, *Plasma Physics and Controlled Nuclear Fusion Research 1994* (IAEA, Vienna, 1996), Vol. 3, p. 323.
[19] X. Garbet, Fusion Sci. Technol. **53**, 348 (2008).
[20] A. E. Hubbard, Plasma Phys. Controlled Fusion **42**, A15 (2000).
[21] M. N. Rosenbluth, private communication (2003).
[22] J. B. Taylor, J. W. Connor, and P. Helander, Phys. Plasmas **5**, 3065 (1998).

[23]M. G. Shats, W. M. Solomon, and H. Xia, Phys. Rev. Lett. **90**, 125002 (2003).
[24]S. I. Itoh, K. Itoh, and S. Toda, Phys. Rev. Lett. **89**, 215001 (2002).
[25]V. B. Lebedev, P. H. Diamond, I. Gruzinova, and B. A. Carreras, Phys. Plasmas **2**, 3345 (1995).
[26]J. W. Connor and H. R. Wilson, Plasma Phys. Controlled Fusion **42**, R1 (2000).
[27]P. B. Snyder, H. R. Wilson, J. R. Ferron, L. L. Lao, A. W. Leonard, T. H. Osborne, and A. D. Turnbull, Phys. Plasmas **9**, 2037 (2002).
[28]C. S. Chang, S. Klasky, J. Cummings, R. Samtaney, A. Shoshani, L. Sugiyama, D. Keyes, S. Ku, G. Park, S. Parker, N. Podhorszki, H. Strauss, H. Abbasi, M. Adams, R. Barreto, G. Bateman, K. Bennett, Y. Chen, E. D'Azevedo, C. Docan, S. Ethier, E. Feibush, L. Greengard, T. Hahm, F. Hinton, C. Jin, A. Khan, A. Kritz, P. Krsti, T. Lao, W. Lee, Z. Lin, J. Lofstead, P. Mouallem, M. Nagappan, A. Pankin, M. Parashar, M. Pindzola, C. Reinhold, D. Schultz, K. Schwan, D. Silver, A. Sim, D. Stotler, M. Vouk, M. Wolf, H. Weitzner, P. Worley, Y. Xiao, E. Yoon, and D. Zorin, J. Phys.: Conf. Ser. **125**, 012042 (2008).
[29]R. J. Colchin, M. J. Schaffer, B. A. Carreras, G. R. McKee, R. Maingi, T. N. Carlstrom, D. L. Rudakov, C. M. Greenfield, T. L. Rhodes, E. J. Doyle, N. H. Brooks, and M. E. Austin, Phys. Rev. Lett. **88**, 255002 (2002).
[30]H. Zohm, Plasma Phys. Controlled Fusion **38**, 105 (1996).
[31]R. E. Waltz, R. L. Dewar, and X. Garbet, Phys. Plasmas **5**, 1784 (1998).
[32]I. Gruzinov, P. H. Diamond, and M. N. Rosenbluth, Phys. Rev. Lett. **89**, 255001 (2002).
[33]R. J. Groebner, M. A. Mahdavi, A. W. Leonard, T. H. Osborne, G. D. Porter, R. J. Colchin, and L. W. Owen, Phys. Plasmas **9**, 2134 (2002).
[34]R. J. Groebner, 19th IAEA Fusion Energy Conference, Lyon, France, Paper No. IAEA-CN-94/EX/C2-3 (2002).
[35]I. Gruzinov, P. H. Diamond, and M. N. Rosenbluth, Phys. Plasmas **10**, 569 (2002).